

Instance, Scale, and Teacher Adaptive Knowledge Distillation for Visual Detection in Autonomous Driving

Qizhen Lan  and Qing Tian 

Abstract—Efficient visual detection is a crucial component in self-driving perception and lays the foundation for later planning and control stages. Deep-networks-based visual systems achieve state-of-the-art performance, but they are usually cumbersome and computationally infeasible for embedded devices (e.g., dash cams). Knowledge distillation is an effective way to derive more efficient models. However, most existing works target classification tasks and treat all instances equally. In this paper, we first present our Adaptive Instance Distillation (AID) method for self-driving visual detection. It can selectively impart the teacher’s knowledge to the student by re-weighing each instance and each scale for distillation based on the teacher’s loss. In addition, to enable the student to effectively digest knowledge from multiple sources, we also propose a Multi-Teacher Adaptive Instance Distillation (M-AID) method. Our M-AID helps the student to learn the best knowledge from each teacher w.r.t. certain instances and scales. Unlike previous KD methods, our M-AID adjusts the distillation weights in an instance, scale, and teacher adaptive manner. Experiments on the KITTI, COCO-Traffic, and SODA10 M datasets show that our methods improve the performance of a wide variety of state-of-the-art KD methods on different detectors in self-driving scenarios. Compared to the baseline, our AID leads to an average of 2.28% and 2.98% mAP increases for single-stage and two-stage detectors, respectively. By strategically integrating knowledge from multiple teachers, our M-AID method achieves an average of 2.92% mAP improvement.

Index Terms—Instance adaptive distillation, knowledge distillation, multi-teacher learning, self-driving visual perception.

I. INTRODUCTION

IN RECENT years, deep learning (DL) has revolutionized many fields, including autonomous driving perception [1], [2], [3], [4], [5], [6], [7], [8]. However, high-performance deep models usually come with large memory footprints and high computational requirements, which makes them impractical for mobile devices (e.g., dash cams). As a result, many DL-based self-driving vehicles have a full trunk of servers, which does not only require a lot of power, but also increases the response

latency. Knowledge Distillation (KD) is a way to overcome such efficiency issues. It can derive a high-performance and lightweight student model by mimicking the knowledge from a powerful and sophisticated teacher model. In the past few years, many KD methods [9], [10] have been explored, and promising results have been achieved in classification problems. However, only a limited number of studies have attempted to apply KD to more challenging visual detection tasks, especially for autonomous vehicles. In object detection KD, most methods investigate what types of knowledge should be mimicked, like feature maps [11], [12], head soft prediction [13], attention-guided feature maps [14], [15], or relation between bounding boxes [16]. They usually treat all examples equally when transferring knowledge of location and category from the teacher to the student. However, due to the uneven quality and difficulty of the examples, teacher models do not learn the instances¹ equally well. Thus, the quality of knowledge provided by teachers varies with the instance. We argue that the distillation weight should adaptively change based on different instances. Sample reweighting is an effective training method in machine learning. Some studies [17], [18], [19], [20] have used hard mining to improve model performance in object detection. However, the hard mining idea in object detection has shown to be unsuitable when it comes to knowledge distillation [21]. Zhang et al. [21] add an auxiliary task branch to the student model, and the variance of the features from that extra branch, which they called data uncertainty, is utilized for reweighing image instances.

In this paper, we first present our Adaptive Instance Distillation (AID) method that reweights distilled instances based on teacher-judged difficulty. In contrast to Zhang et al. [21], our AID does not rely on student auxiliary features’ uncertainty because the variance of auxiliary features may not always represent the distillation utility of an instance, and it results in additional computation. More importantly, we argue that the importance of instances should not be determined by the feature statistics of the student network but rather by the teacher’s prediction. Our AID reweights an instance based on the teacher’s original loss, which reflects the reliability of the teacher on that instance. Specifically, an instance with a larger teacher’s prediction loss will receive small distillation weights and thus less attention from the student model. In other words, our AID allows the

Manuscript received 22 August 2022; revised 27 September 2022; accepted 10 October 2022. This work was supported by the National Science Foundation (NSF) under Grant 2153404. (Corresponding author: Qing Tian.)

The authors are with the Department of Computer Science, Bowling Green State University, Bowling Green, OH 43403 USA (e-mail: qlan@bgsu.edu; qtian@bgsu.edu).

Color versions of one or more figures in this article are available at <https://doi.org/10.1109/TIV.2022.3217261>.

Digital Object Identifier 10.1109/TIV.2022.3217261

¹In our KD scenario, ‘instance’ means ‘image example’ by default.

84 student to learn more from the teacher on instances where the
 85 teacher performs well while giving the student more freedom to
 86 learn “teacher-uncertain” instances on their own.

87 We also argue that multiple teachers can be more beneficial
 88 than a single teacher and that knowledge distillation should be
 89 scale-aware. Few works [22], [23] in KD have adopted the idea
 90 of adaptive reweighting in a multi-teacher framework. Both
 91 You et al. [22] and Liu et al. [23] are designed for relatively
 92 simple classification tasks and they are not scale-aware. It is not
 93 easy to apply those classification distillation methods to more
 94 challenging detection tasks because the dimensionality of the
 95 soft targets often varies with the structure of the detection heads.
 96 You et al. [22] use fixed weights to combine predictions from
 97 multiple teachers. However, fixed weights cannot adaptively
 98 distinguish high-quality teachers from low-quality teachers. Liu
 99 et al. [23] weigh the teachers based only on their intermediate
 100 features, without considering the features’ quality (whether they
 101 lead to correct prediction). This label-free method can easily lead
 102 student training astray.

103 In the multi-teacher distillation scenario, each teacher has
 104 different judgments about an instance and a scale, and it is crucial
 105 for the student to determine which teacher’s knowledge is more
 106 valuable. We point out that knowledge distillation should focus
 107 on not only what kind of knowledge to imitate, but also on which
 108 instance/scale, and from which teacher comes more valuable
 109 knowledge. Specifically, knowledge from instances/scales that
 110 a teacher can accurately predict should be identified and trans-
 111 ferred to the student with emphasis, while the student should
 112 avoid paying too much attention to instances/scales where the
 113 teacher has no expertise.

114 In this paper, as an extension to AID, we propose a Multi-
 115 teacher Adaptive Instance Distillation (M-AID) framework. Our
 116 M-AID allows a student to choose the best knowledge from
 117 each teacher w.r.t. certain instances/scales. To our best knowl-
 118 edge, it is the first exploration of multi-teacher KD for object
 119 detection, especially in autonomous driving scenarios. Guided
 120 by our M-AID, a student can learn from a group of experts with
 121 each excelling in a particular area (a certain set of instances and
 122 scales). Thus, the risk of the student being misled by unreliable
 123 instances, scales, and teachers can be greatly reduced. There-
 124 fore, the distilled visual detectors by our methods can be more
 125 accurate and safer when deployed on automated vehicles.

126 In summary, the contributions of this paper can be summarized
 127 as follows:

- 128 • We present our Adaptive Instance Distillation (AID)
 129 method that allows a student to discern the reliability of
 130 the teacher’s knowledge on a per-instance basis according
 131 to the teacher’s performance.
- 132 • We are the first to introduce a multi-teacher distillation
 133 framework for self-driving visual detection or visual detec-
 134 tion in general. Our M-AID guides the student to selectively
 135 learn more from more knowledgeable teachers w.r.t. an
 136 instance and a scale, rather than blindly learn from all
 137 instances and all scales equally. When all the teachers’
 138 knowledge is unreliable, the student has to rely on itself. A
 139 group of teachers with different sets of expertise are shown
 140 to benefit student learning.

- Our methods advance the state-of-the-art of visual detec-
 141 tion in autonomous driving. Our AID has achieved 2.75%,
 142 2.61% and 1.3% average mAP improvement on the KITTI,
 143 COCO-Traffic, and SODA10 M datasets, respectively. The
 144 proposed M-AID has improved the average mAP by 2.95%
 145 and 2.91% on KITTI and COCO-Traffic, respectively.

146 It is worth noting that this journal paper extends our previous
 147 work [24] significantly by: (1) proposing a new multi-teacher
 148 adaptive instance distillation (M-AID) framework that allows
 149 the student model to selectively absorb knowledge from multiple
 150 sources. (2) Our M-AID is adaptive to instance, scale, and
 151 teacher. It can significantly improve the distillation performance
 152 of our AID and other competing approaches for visual detec-
 153 tion in self-driving vehicles. (3) We have experimented with
 154 more competing approaches (including [11], [12], [13], [15],
 155 [16], [21], [25], [26]), new backbones (ResNet-18, and Mo-
 156 bileNetV2 [27]), and a new intelligent-vehicle-related dataset
 157 (SODA10M [28]). (4) we have also visualized different models’
 158 attention saliency maps for better understanding their differ-
 159 ences. (5) Finally, we point out or address some typos in [24]: 1.
 160 In [24]’s Fig. 3 caption, the first prediction result is by the student
 161 baseline model (as indicated in the text), not the teacher baseline
 162 model; 2. “teacher confidence” is loosely defined; 3. In the
 163 discussion of focal loss [17] in the related work section of [24],
 164 “low cross-entropy,” not “high cross-entropy,” corresponds to
 165 “easy” samples (e.g., most backgrounds); 4. We have also fixed
 166 some reference and expression issues of [24].

II. RELATED WORKS

168 This section reviews the most relevant works in the areas
 169 of Visual Object Detection, Adaptive Sample Weighting, and
 170 Knowledge Distillation.

A. Visual Object Detection

172 Efficient visual detection is critical to self-driving perception,
 173 which lays the foundation for self-driving planning, control, and
 174 coordination. In fact, some intelligent car makers like Tesla
 175 even commit to the pure vision approach for their autopilot
 176 products [29], [30]. Compared to traditional object detectors
 177 like [31], [32], detectors based on deep convolutional networks
 178 have received more and more attention. Deep object detec-
 179 tion models can be categorized into two-stage [33], [34], [35],
 180 anchor-based one-stage [17], [20], [36], [37], and anchor-free
 181 one-stage [38], [39], [40], [41] detectors. The two-stage de-
 182 tectors employ a region proposal network (RPN) to generate
 183 a set of proposals for potential foreground objects and then
 184 classify and localize the selected proposed regions for final
 185 prediction. In contrast, one-stage detectors perform classifica-
 186 tion and localization directly without proposals for regions of
 187 interest. They can achieve high efficiency compared to two-stage
 188 detectors. Anchor-based one-stage detectors need to traverse a
 189 large number of anchor boxes to find possible matches for the
 190 ground truth objects, adding to the computational burden. The
 191 anchor-free detectors [38], [39], [40], [41] directly predict an
 192 object’s center point or key-points from feature maps, which
 193 reduces the computational cost and achieves promising results

195 compared to anchor-based one-stage detectors. Although different
 196 detectors may have various detection heads and losses, most
 197 state-of-the-art detectors adopt the well-known FPN idea [42] or
 198 its variants like [43] to improve the detection ability on different
 199 scales. Deep detectors normally come with high computational
 200 and storage costs, which constrain their wide deployment on
 201 intelligent vehicles.

202 *B. Adaptive Sample Weighting*

203 Adaptive sample (e.g., bounding box, image,...) weighting
 204 by adjusting the contributions of each sample can help with
 205 effective learning in object detection. “Hard mining” is one
 206 reweighting technique that puts non-uniform attention to sam-
 207 ples based on difficulty. In object detection, hard-mining plays a
 208 critical role in improving detection performance [17], [18], [19],
 209 [20]. It helps reduce the relative weight of simple samples (e.g.,
 210 most background bounding boxes) and gives more attention
 211 to difficult ones. However, the idea of hard mining is proved
 212 to be less effective in knowledge distillation [21]. In contrast,
 213 down-weighting hard samples or paying more attention to easy
 214 ones leads to better performance distilled models. One important
 215 question to ask is: how should the sample difficulty/importance
 216 be measured? In object detection, Lin et al. [17] use modified
 217 cross-entropy loss (a.k.a. focal loss) to measure the difficulty of
 218 bounding boxes. Bounding boxes with high prediction probabili-
 219 ty of the correct class (e.g., most backgrounds) are considered
 220 to be easy and they receive even less attention compared to
 221 the unmodified cross entropy case. GHM-C in [18] follows a
 222 similar idea to focal loss. Cao et al. [19] use Hierarchical Local
 223 Ranks to compute image sample importance in mini-batches.
 224 In knowledge distillation, Zhang et al. [21] measure image
 225 sample importance through feature variance of an auxiliary
 226 branch added to the student model. As in [21], our method
 227 applies instance reweighting during knowledge distillation on
 228 the image level. However, unlike previous approaches, we utilize
 229 the teacher network’s prediction losses to determine instance
 230 importance for the student.

231 *C. Knowledge Distillation*

232 Knowledge distillation (KD) was introduced by Hinton
 233 et al. [9]. The goal of KD is to train a high-performance light-
 234 weight student model by transferring a powerful teacher model’s
 235 knowledge. It can help meet the high accuracy and low com-
 236 plexity requirements of autonomous driving vehicles. The type
 237 of distilled knowledge can be categorized into three different
 238 forms: feature-based [11], [12], [14], [15], [44], [45], [46], [47],
 239 [48], response-based [9], [13] and relation-based [16], [49], [50].
 240 The main difference lies in the kind of knowledge transferred.
 241 Unlike distillation for classification, knowledge distillation for
 242 object detection is a more challenging task. As a result, KD is
 243 less explored in object detection than in classification tasks.

244 It was not until 2017 that Chen et al. [51] first proposed
 245 their KD method for object detection. To deal with the high
 246 foreground-background imbalance in object detection, Chen
 247 et al. [51] down-weight the background distillation loss in the
 248 classification head.

249 Nguyen et al. [25] propose a label assignment distillation
 250 method, where the teacher’s encoded labels are used to train
 251 a student. However, this KD method is only applied to the
 252 Probabilistic Anchor Assignment (PAA) [26] detector and is
 253 hard to generalize to other detectors. Hao et al. [52] introduce
 254 an auxiliary network to estimate the label assignment function
 255 to supervise intermediate layer training. However, the auxiliary
 256 network requires extra computation, and the distillation
 257 performance highly depends on the design of the auxiliary
 258 network. Zhang et al. [14] propose to utilize an attention-guided
 259 method to improve the distillation results. Wang et al. [11]
 260 consider only imitating the features near ground truth boxes.
 261 Yang et al. [15] treat all background features as noise and only
 262 focus attention on the foregrounds. In contrast, Guo et al. [12]
 263 decouple foreground and background features and distill them
 264 using different weights. Dai et al. [16] locate distinctive areas
 265 for distillation through finding places where the prediction gap
 266 between the teacher and the student is large. Those feature-based
 267 KD methods [11], [12], [14], [15] assign different weights to
 268 target pixels based on whether they belong to the foreground or
 269 the background. Nevertheless, the foreground-and-background
 270 assignment is meticulously determined in a subjective manner
 271 with the help of the ground truth. It follows that some
 272 informative areas could potentially be ignored and some less
 273 important locations could receive too much attention. Zheng
 274 et al. [13] develop the idea of generalized focus detectors [53]
 275 to enable students to mimic the teacher’s localization soft-logits
 276 knowledge to improve their performance. However, it does not
 277 consider the different quality of teacher’s prediction like our
 278 approach, and it can only be applied to the single-stage detectors
 279 with GFL [53]. All the above works [11], [12], [13], [14], [15],
 280 [16], [25], [52] have a common issue: they do not consider the
 281 teachers’ prediction ability on different instances. It follows
 282 that when the teacher is wrong about certain instances, those
 283 distillation methods can no longer provide valuable knowledge
 284 to the student. Or even worse, they can mislead the student
 285 learning. Deng et al. [54] apply KD to video-based object
 286 detection. Zeni et al. [55] is focused on weakly supervised
 287 object detection. Both are interesting directions, but they are
 288 beyond the scope of this paper.

289 To the best of our knowledge, there is only one work [21]
 290 that attempts to apply the idea of instance-based reweighting to
 291 the domain of distillation. They add an auxiliary task branch to
 292 the student model and utilize the variance of its feature maps to
 293 measure the importance of a sample. They give larger weights
 294 to samples with low variances. However, there is no enough
 295 justification why auxiliary feature variance and sample impor-
 296 tance are related. In contrast to Zhang et al. [21] that uses the
 297 student network’s information to measure instance weight, we
 298 leverage the teacher’s prediction for each instance to calculate
 299 the reliability of the distilled knowledge.

300 Most detection KD works follow a one-to-one distillation
 301 paradigm. Multi-teacher distillation methods have been applied
 302 in a limited number of studies for classification tasks [22], [23],
 303 [56], [57], [58]. You et al. [22] and Fukuda et al. [57] assign
 304 a uniform or fixed weight to each teacher and each instance,
 305 which cannot adaptively differentiate teachers and instances.

306 Liu et al. [23] use a latent factor to represent a teacher's intermediate features to measure their importance. However, this
 307 label-free method can mislead the student training when teachers produce a wrong prediction. Du et al. [58] use multi-objective
 308 optimization in the gradient space to derive teacher importance
 309 weights. However, their weighting method does not consider a
 310 teacher's prediction performance on a certain instance. As a result,
 311 the student can be misled by low-quality teacher prediction.
 312 Some studies [59], [60], [61], [62] try to let different students learn from each other to derive a high-performance model by
 313 ensemble methods. They are orthogonal/complimentary to the
 314 multi-teacher paradigm and are beyond the scope of this paper.
 315

316 What's more, all the previous methods [22], [23], [56], [57],
 317 [58], [59], [60], [61], [62] are focused on classification tasks.
 318 Things become more complicated when it comes to knowledge
 319 distillation for object detection. For example, we must take
 320 into account the head architecture variations across different
 321 teachers and students. Also, we need to consider the different
 322 foreground-background assignment, bounding box regression,
 323 and classification methods between the teachers and the student.
 324 In this paper, targeting visual detection in autonomous driving,
 325 we propose multi-teacher adaptive instance distillation (M-AID)
 326 method to guide the student to learn more from more knowledge-
 327 able teachers on more useful scales and instances. To the best of
 328 our knowledge, our M-AID is the first multi-teacher distillation
 329 framework for object detection, especially in the autonomous
 330 driving domain. Our M-AID evaluates the quality of different
 331 teachers' knowledge based on their predictions and helps the
 332 student to learn more valuable knowledge across different scales
 333 and instances.

III. METHODOLOGY

336 Object detection involves multiple tasks, e.g., bounding box
 337 regression, category classification, and objectness prediction.
 338 Therefore, knowledge distillation for object detection is more
 339 complex than for classification. To deal with the imbalance
 340 problem between the foreground and background, many adaptive
 341 weighting strategies, such as hard mining [17], have been
 342 proposed. However, Zhang et al. [21] show that hard image
 343 instance mining does not work well in knowledge distillation.
 344 Instead, they use an auxiliary task branch to estimate uncertainty
 345 in the data and make students pay more attention to the 'stable'
 346 samples. However, the variety of the auxiliary features is not
 347 necessarily a reliable indicator for image instance importance,
 348 and it does not reflect the importance of the knowledge from the
 349 teacher. In contrast to their approach, we propose to measure
 350 the value of the teacher's knowledge on a per-instance basis by
 351 calculating the gap between the ground truth and the teacher's
 352 prediction. In other words, if the teacher model cannot predict
 353 an example well, it implies that the teacher's knowledge about
 354 that instance is less trustworthy. On the other hand, valuable
 355 knowledge comes from those instances that can be accurately
 356 predicted by the teacher model. The student network should
 357 pay more attention to such instances. In addition, we propose to
 358 employ multiple teachers to allow students to selectively absorb
 359 knowledge from multiple sources. The two approaches (AID
 360 and M-AID) will be detailed in the following two subsections.

A. Adaptive Instance Knowledge Distillation

361 In general, knowledge distillation tasks have two kinds of
 362 losses. One is the distillation loss $\mathcal{L}_{distill}$ which measures the
 363 knowledge (or prediction) difference between the student and the
 364 teacher model. The other one is the task loss, which is used to
 365 guide the student to learn the original task. In this paper, we first
 366 present our Adaptive Instance distillation (AID) to adaptively
 367 distill the knowledge of the teacher model on a per-instance
 368 basis for object detection tasks. The idea is that the student model
 369 should pay more attention to instances in which the teacher has
 370 more authority/trustworthiness rather than learn all instances
 371 equally from the teacher model. Fig. 1 illustrates how our AID
 372 guides the student model to better learn the most valuable and
 373 reliable knowledge from the teacher.

374 We define the overall loss for student learning as:

$$\mathcal{L}_i^S = \mathcal{L}_{task,i}^S + \lambda \mathcal{L}_{AID,i}^{S,T}. \quad (1)$$

375 where i indicates the i -th instance. The superscripts S and T
 376 imply that a corresponding loss term depends on the student
 377 and/or the teacher prediction. λ is a weighting factor balancing
 378 the contribution between the task loss \mathcal{L}_{task} and our instance
 379 adaptive distillation loss \mathcal{L}_{AID} . The latter is defined as follows:

$$\mathcal{L}_{AID,i}^{S,T} = \exp^{-\alpha \mathcal{D}_i^T} \mathcal{L}_{distill,i}^{S,T}, \quad (2)$$

380 where

$$\mathcal{D}_i^T = \mathcal{L}_{task,i}^T \quad (3)$$

381 is the teacher's object detection task loss, i.e., the distance
 382 between the ground truth and the prediction, on the i -th instance.
 383 α is a hyper-parameter that needs to be tuned empirically (we
 384 set it to 0.1 in all our experiments). As we can see from Eq. (2),
 385 the adaptive weight of the instance i has a negative exponential
 386 correlation with the teacher's prediction loss. The larger the
 387 teacher's error on a certain instance i (i.e., \mathcal{D}_i^T) is, the smaller
 388 weight or less attention the instance i will receive from the
 389 student model during the knowledge distillation process. On the
 390 other hand, instances where the teacher predicts accurately (i.e.,
 391 with smaller \mathcal{D}_i^T values) deserve more of the student's attention
 392 in the knowledge transfer process. The instance weight degrades
 393 exponentially with the increase of the teacher's prediction error.
 394 The exponential function sets an appropriate range of the punishment.
 395 Take the extreme cases for example. An instance where the
 396 teacher's loss is extremely large will receive approximately zero
 397 attention while there will be no knowledge transfer degradation
 398 for instances where the teacher model makes 'perfect' prediction
 399 (zero task loss).

400 Putting all things together, the final loss for our instance-
 401 adaptive student learning will be:

$$\mathcal{L}_i^S = \mathcal{L}_{task,i}^S + \lambda \exp^{-\alpha \mathcal{L}_{task,i}^T} \mathcal{L}_{distill,i}^{S,T}. \quad (4)$$

402 It is worth noting that Feature Pyramid Networks (FPN) [42]
 403 or its variants have been widely adopted by state-of-the-art
 404 object detectors. To improve knowledge transfer for objects of
 405 different scales, we can apply our AID strategy to each output
 406 layer of the FPN (Fig. 1). In this case, our AID adaptively
 407 weighs not only the instance-wise knowledge but also scale-wise
 408 feature knowledge during the knowledge distillation process.

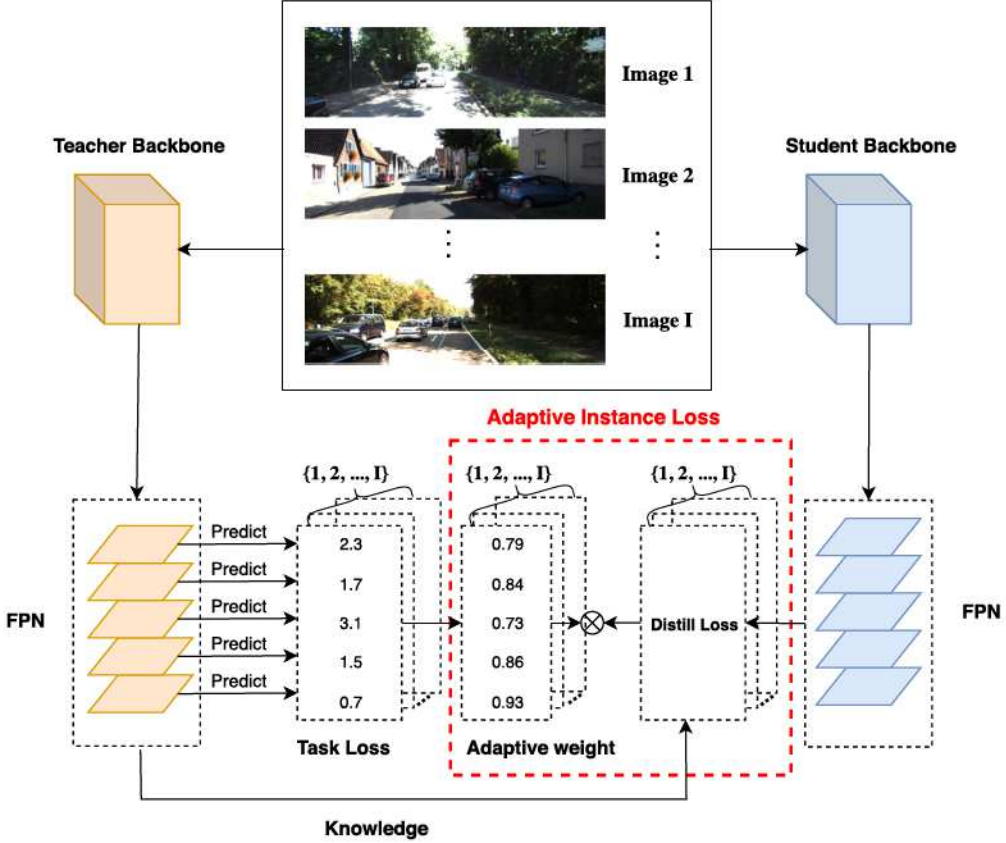


Fig. 1. Illustration of the proposed adaptive instance distillation (AID) method. The teacher losses associated with different instances and scales will be transformed into weights to guide the knowledge distillation process. The transformation is based on (2). I is the total number of images.

411 The student will rely more on the teacher for scales where
 412 the teacher feels more confident.² For scales where the teacher
 413 performs bad, the student will rely more on itself to learn instead
 414 of being misled by the teacher. Such scale-adaptive knowledge
 415 distillation contributes to better object detection on different
 416 scales. In the case of autonomous driving, a car can better detect
 417 road objects of different sizes and distances. More details will
 418 follow in the experiment section.

419 B. Multi-Teacher Adaptive Instance Distillation

420 Most successful knowledge distillation methods are based
 421 on the one-to-one framework, where one teacher teaches one
 422 student. As an old Chinese saying goes: ‘In a party of three,
 423 there must be one whom I can learn from.’ Some multi-teacher
 424 knowledge distillation methods [22], [56], [58] have been pro-
 425 posed and proven to be beneficial for classification tasks. They
 426 combine predictions from multiple teachers with fixed weight
 427 assignments or with gradient weighting schemes [58]. However,
 428 fixed weights cannot adaptively distinguish high-quality teach-
 429 ers from low-quality teachers, while the gradient-based weight-
 430 ing method [58] may easily mislead the student by low-quality
 431 teachers. In this paper, we propose Multi-teacher Adaptive In-
 432 stance Distillation (M-AID) method to assign different weights

433 to different teachers in a dynamic manner. By combining the
 434 strategy with our instance-and-scale-aware AID, we can adap-
 435 tively select valuable knowledge for the student across different
 436 instances, scales, and teachers.

437 Fig. 2 illustrates how M-AID works. The two main types of
 438 losses for our multi-teacher framework are as follows:

$$\mathcal{L}_i^S = \mathcal{L}_{task,i}^S + \lambda \sum_{k=1}^K w_{k,i} \mathcal{L}_{AID,k,i}^S, \quad (5)$$

439 where $\mathcal{L}_{task,i}^S$ is the original detection task loss of the student,
 440 and k in $\mathcal{L}_{AID,k,i}$ stands for the k -th teacher. One difference
 441 between Eq. (1) and Eq. (5) is that adaptive distillation loss
 442 $\mathcal{L}_{AID,k,i}$ is weighted by $w_{k,i}$, which is defined as:

$$w_{k,i} = \frac{\exp^{-\mathcal{D}_{k,i}^T}}{\sum_{k=1}^K \exp^{-\mathcal{D}_{k,i}^T}}, \quad (6)$$

443 where $\mathcal{D}_{k,i}^T$ is the k -th teacher’s object detection task loss, i.e.,
 444 the distance between the ground truth and the prediction, on the
 445 i -th instance. The purpose of the denominator in Eq. (6) is to
 446 normalize the distillation losses of multiple teachers.

²here, confident is loosely defined as knowledgeable

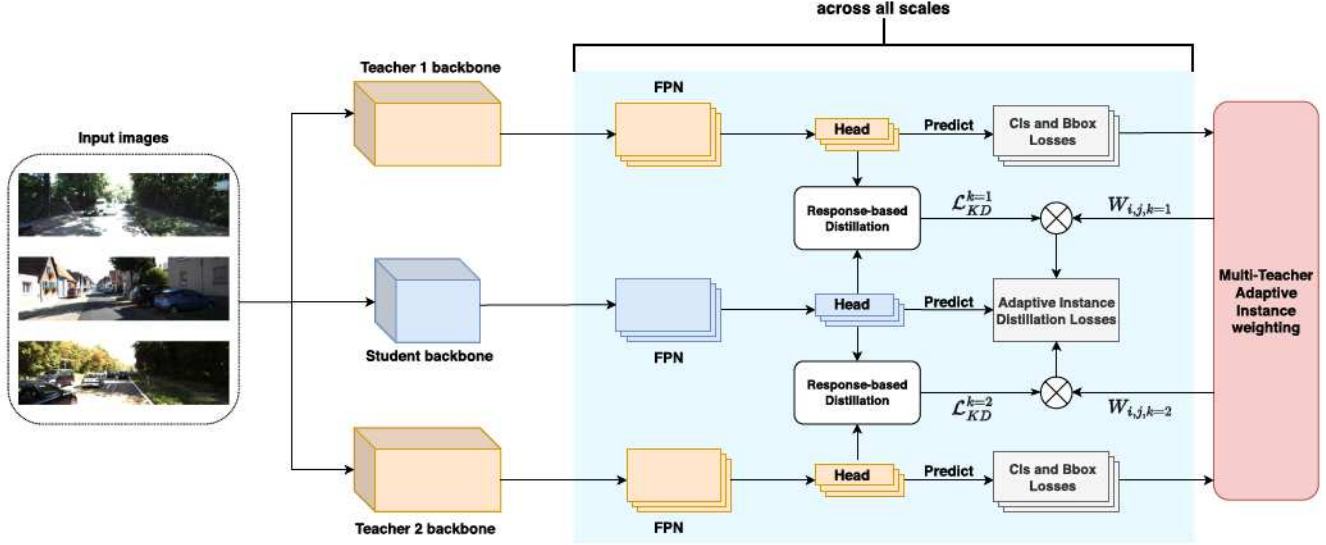


Fig. 2. Illustration of the proposed multi-teacher adaptive instance distillation (M-AID) method. The losses associated with the k th teacher's prediction for the j th scale of the i th instance will be transformed into weights $W_{i,j,k}$ to reweight distillation losses, which directs more student attention to more valuable knowledge across different instances, scales, and teachers. Without loss of generality, only two teachers are shown in this figure.

447 Putting all things together, we define the loss of our M-AID
 448 distilled student as:

$$\mathcal{L}_i^S = \mathcal{L}_{task,i}^S + \lambda \frac{\exp^{-\mathcal{L}_{task,k,i}^T}}{\sum_K \exp^{-\mathcal{L}_{task,k,i}^T}} \exp^{-\alpha \mathcal{L}_{task,k,i}^T} \mathcal{L}_{distill,k,i}^{S,T} \quad (7)$$

449 The *task* in $\mathcal{L}_{task,k,i}$ includes category classification and
 450 bounding box regression. Re-weighting according to the two
 451 subtask losses are conducted separately in our M-AID.

452 IV. EXPERIMENTAL SETUP AND RESULTS

453 A. Datasets

454 To evaluate our methods, we utilize three autonomous driving
 455 related datasets in our experiments.

456 **KITTI** [63] is a 2D-object detection dataset that includes
 457 seven different types of road objects. As suggested in [64], we
 458 group similar categories into one. Specifically, we perform the
 459 following modification to the original KITTI dataset:

- 460 • Car \leftarrow car, van, truck, tram
- 461 • Pedestrian \leftarrow pedestrian, person
- 462 • Cyclist \leftarrow cyclist

463 It includes 7481 images with annotations. We split it into a
 464 training set and a validation set in the ratio of 8:2.

465 **COCO-Traffic** is a dataset containing 13 traffic-related cat-
 466 egories. This dataset is obtained by selecting categories related
 467 to self-driving from MS COCO 2017 [65]. The COCO-Traffic
 468 dataset includes the following categories:

- 469 • **Road-related:** bicycle, car, motorcycle, bus, train, truck,
 traffic light, fire hydrant, stop sign, parking meter
- 470 • **Others:** person, cat, dog

471 Unlike [24], we keep only images containing at least one
 472 road-related object to filter out those images that only contain
 473 indoor objects. The selection is applied to both the training and
 474 validation sets.

475 **SODA10 M** [28] is a recent large-scale 2D dataset, which
 476 contains 10 M unlabeled images and 20 k labeled images from
 477 6 object categories (i.e., *Pedestrian*, *Cyclist*, *Car*, *Truck*, *Tram*,
 478 and *Tricycle*). At the time of writing, SODA10 M is the largest
 479 public autonomous driving dataset that can be used for 2D visual
 480 detection.

481 B. Implementation Detail

482 1) *Adaptive Instance Distillation*: In our AID experiments,
 483 we chose Faster-RCNN [33] as an example of two-stage detec-
 484 tors, and selected Generalized Focal Loss (GFL) [53] and Prob-
 485abilistic anchor assignment (PAA) [26] as examples of single-
 486 stage detectors. All teachers have a ResNet101 [66] backbone.
 487 We experimented with three different student backbone archi-
 488 tectures (i.e., ResNet-50, ResNet-18, and MobileNetsV2). We
 489 re-implemented the following state-of-the-art KD methods [11],
 490 [12], [13], [14], [15], [16], [21], [25] to compare with our AID:

- 491 • Attention-Guided by Zhang et al. [14] (ICLR'21)
- 492 • GI-imitation by Dai et al. [16] (CVPR'21)
- 493 • DeFeat by Guo et al. [12] (CVPR'21)
- 494 • FGD by Yang et al. [15] (CVPR'22)
- 495 • LD by Zheng et al. [13] (CVPR'22)
- 496 • Fine-Grained by Wang et al. [11] (CVPR'19)
- 497 • PAD by Zhang et al. [21] (ECCV'20)
- 498 • LAD by Nguyen et al. [25] (WACV'22)

499 For a fair comparison, all re-implemented KD methods and
 500 our AID are imposed on multi-level FPN (P3-P7). In our experi-
 501 ments, the competing instance adaptive KD method, PAD [21], is
 502 applied on top of Attention-Guided [14]. In the implementation
 503 of our AID, we use the sum of the teacher's classification losses
 504 and bounding box losses to re-weigh the KD losses. The teacher
 505 and student baseline models (without any KD) were directly
 506 trained with MMDetection [67]'s default configuration.

507 2) *Multi-Teacher Adaptive Instance Distillation*: In our M-
 508 AID experiments, we take Zheng et al. [13]'s response-based

TABLE I
PERFORMANCE (MAP) OF DIFFERENT DISTILLATION METHODS WITH GFL DETECTOR [53] ON THE KITTI AND COCO TRAFFIC DATASETS

KD methods	Student backbones		ResNet-50		ResNet-18	
	KITTI	COCO Traffic	KITTI	COCO Traffic	KITTI	COCO Traffic
Teacher (w ResNet-101)	89.4	71.8	89.4	71.8		
Student-baseline	85.1	67.7	81.9	61.9		
PAD-attention-Guided [21]	84.7	63.6	80.8	60.7		
Attention-Guided [14]	86.4	69.5	84.4	62.6		
Attention-Guided + AID	88.0	70.1	84.7	64.1		
GI-imitation [16]	86.1	69.3	84.6	63.7		
GI-imitation + AID	87.9	69.6	85.2	64.6		
DeFeat [12]	85.4	69.3	83.3	62.7		
DeFeat + AID	86.4	69.5	84.7	63.8		
LD [13]	85.5	67.8	83.6	62.7		
LD + AID	87.2	68.4	83.8	64.4		
FGD [15]	89.2	71.0	86.7	65.9		
FGD + AID	89.9	71.1	87.5	66.4		
Fine-Grained [11]	84.4	68.6	82.6	62.4		
Fine-Grained + AID	86.6	69.1	84.4	62.9		

Note: The teacher model and the student-baseline are non-distillation GFL models with ResNet-101 and ResNet-50/18 as backbones, respectively.

510 approach (LD) as a KD baseline, upon which we apply our
511 instance, scale, and teacher adaptive knowledge reweighting
512 methods. All the student models use ResNet-50 or ResNet-18 as
513 the backbone and GFL [53] as the head. For those teacher models
514 that do not have GFL [53], we implement GFL in their heads to
515 ensure the feasibility of multi-teacher distillation.³ Since the two
516 distillation losses (one for classification and one for bounding
517 box regression) are separated in LD [13], we apply AID and
518 M-AID to the two losses separately.

519 *3) Hyperparameters:* All the detection experiments are con-
520 ducted in the MMDetection framework [67] using Pytorch [68].
521 We do not perform much hyperparameter tweaking. In our
522 re-implementation of the state-of-the-art KD methods [11], [12],
523 [14], [15], [16], [25], we adopt the same hyperparameter values
524 as provided by their authors. As for LD [13], we set both
525 classification distillation and localization distillation weights to
526 0.05 and make slight adjustments based on different detectors
527 and datasets. Furthermore, we set $\alpha = 0.1$ in Eq. (2) for our AID
528 and M-AID throughout all experiments. All models are suffi-
529 ciently trained to convergence (i.e., 24 epochs for models with
530 ResNet-101 backbone, 12 epochs for models with ResNet-50
531 backbone, ResNet-18, and MobileNetV2).

532 We verify the effectiveness of our proposed AID and M-AID
533 on the autonomous-driving-related KITTI, COCO-Traffic and
534 SODA10M datasets. We present our AID’s and M-AID’s results
535 in Sections IV-C and IV-D, respectively. Also, we will show
536 the intuitive differences in CAM visualization of our approach
537 from other baselines. All models are evaluated in terms of
538 mean averaged precision (mAP) with 0.5 as the Intersection
539 over Union (IoU) threshold.

540 C. Adaptive Instance Distillation (AID) Results

541 *1) Quantitative Analysis:* In this section, we report our AID’s
542 quantitative performance on three state-of-the-art detectors, in-
543 cluding double-stage Faster RCNN, single-stage GFL [53], and
544 PAA [26].

³This ensures the teacher models’ localization heads to have same-dimension generalized logits.

545 We first compare our proposed AID with several state-of-the-
546 art KD methods [11], [12], [13], [14], [15], [16], [21] using the
547 GFL detector. The results are reported in Table I. All teachers
548 have a ResNet-101 backbone, and we test two students (i.e.,
549 one with a ResNet-50 backbone and the other with a ResNet-18
550 backbone). As can be seen from Table I, by applying our AID
551 method, we can achieve consistent improvement over the com-
552 peting KD baselines on the KITTI and COCO-Traffic datasets
553 for both ResNet-50 and ResNet-18 backbones. In particular, with
554 a ResNet-50-backbone student on the KITTI dataset, our AID
555 achieves 2.2% mAP improvement over the Fine-Grained [11]
556 baseline (bottom two rows). Also in the ResNet-50-KITTI case,
557 FGD + AID (third-to-last row) even beats the larger teacher
558 model (with a ResNet-101 backbone). The main reason is that
559 our AID gives the student more freedom to rely on itself to
560 learn when the teacher provides untrustworthy prediction on
561 certain instances/scales. We can also observe a general trend
562 that the improvement brought about by our AID is larger on the
563 smaller ResNet-18 backbone than on ResNet-50. On average,
564 ResNet-50-based students gain 2.57% mAP and 1.93% mAP on
565 KITTI and COCO-Traffic, respectively. Students with ResNet-
566 18 backbones gain an average of 3.15% and 2.47% mAP on the
567 two datasets.

568 Table II shows that our AID outperforms state-of-the-art KD
569 baselines on the Faster-RCNN detector [33] as well. On average,
570 our AID improves student performance by 2.53% mAP and
571 3.43% mAP on the KITTI and COCO-Traffic datasets, respec-
572 tively.

573 Table III demonstrates the results with the PAA detector [26]
574 on another autonomous driving dataset - SODA10M [28]. It can
575 be observed that our AID results in a 1.3% mAP improvements
576 with the more compact MobileNetV2 as backbone.

577 *2) Qualitative Analysis:* Fig. 3 shows a random example on
578 the KITTI dataset. The qualitative results of three GFL models
579 are demonstrated. They are (from top to bottom): 1) teacher
580 GFL model, 2) Zhang et al. [14]’s Attention-Guided model with
581 a ResNet-50 backbone, and 3) our AID-distilled model with a
582 ResNet-50 backbone. For the readers’ convenience, we highlight

TABLE II

PERFORMANCE (MAP) OF DIFFERENT DISTILLATION METHODS WITH FASTER R-CNN DETECTOR [33] ON THE KITTI AND COCO TRAFFIC DATASETS

Student backbones	ResNet-50		ResNet-18	
	KITTI	COCO Traffic	KITTI	COCO Traffic
KD methods				
Teacher (w ResNet-101)	89.3	67.9	89.3	67.9
Student-baseline	88.9	67.5	84.1	63.1
PAD-attention-Guided [21]	88.9	67.6	86.4	68.2
Attention-Guided [14]	89.0	67.8	87.2	65.3
Attention-Guided + AID	89.6	69.0	88.4	68.4
FGD [15]	88.9	67.7	87.0	64.1
FGD + AID	89.5	70.1	88.6	67.4

Note: The teacher model and the student-baseline are non-distillation Faster-RCNN models with ResNet-101 and ResNet-50/18 backbones, respectively.



Fig. 3. Qualitative Analysis on KITTI – From top to bottom, the prediction results are respectively from 1) Teacher baseline model, 2) Zhang et al. [14]’s KD student baseline model, and 3) our AID distilled student model. We have cropped and zoomed in on portions where the models disagree most. The zoomed-in views are alongside each image and unlike the original view, they do not contain category labels and confidence scores for clarity. Best viewed in color and zoomed in.

TABLE III

PERFORMANCE (MAP) OF LAD [25] WITH PAA DETECTOR [26] ON THE SODA10 M DATASETS

Student backbones	MobileNetV2
KD methods	
Teacher (w ResNet-101)	55.2
Student-baseline	49.7
LAD [25]	50.1
LAD + AID	51.0

Note: The teacher model and the student-baseline are non-distillation PAA [26] models with ResNet-101 and MobileNetV2 as backbones, respectively.

583 the prediction differences between our AID-based model and the
 584 other baseline models using cyan boxes and ovals. According to
 585 Fig. 3, generally speaking, our AID-distilled model has better
 586 detection capability for overlapping objects and small-scale ob-
 587 jects. For example, in the top image, the teacher baseline model

generates a bunch of approximate bounding boxes in order to
 588 locate the pedestrian and the car that overlap each other in the
 589 right part of the image. Although Zhang et al. [14]’s distilled
 590 model improves the detection a bit (the middle image), it still
 591 struggles to find the correct bounding boxes for the overlapping
 592 objects. On the other hand, the bounding boxes generated by our
 593 AID-distilled model are more precise. An example showing our
 594 AID’s superiority in detecting small-scale objects can be found
 595 on the left part of the image. Both the teacher model and Zhang
 596 et al. [14]’s Attention-Guided model fail to detect the small-scale
 597 car behind the pole, while our AID-distilled model can detect
 598 the car without any problem.

599 Fig. 4 demonstrates another random example on the COCO-
 600 Traffic dataset. From left to right, the results are respectively
 601 from 1) the Teacher GFL baseline model, 2) Zhang et al. [14]’s
 602 distilled GFL model, and 3) our AID-distilled GFL model. Both

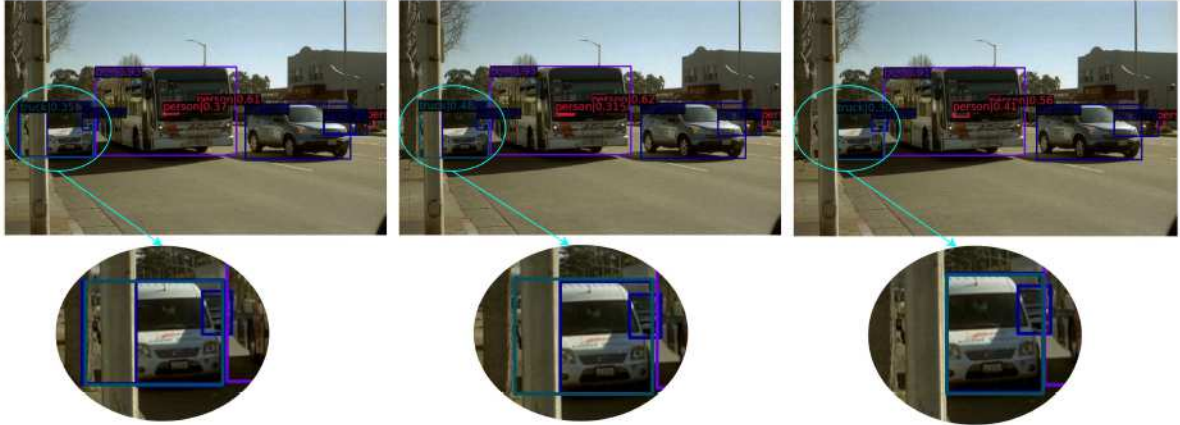


Fig. 4. Qualitative Analysis on COCO traffic – From left to right, the prediction results are respectively from 1) Teacher baseline model, 2) Zhang et al. [14]’s KD student baseline model, and 3) our AID distilled model. We have cropped and zoomed in on portions where the models disagree most. The zoomed-in views are under each image and unlike the original view, they do not contain category labels and confidence scores for clarity. Best viewed in color and zoomed in.

604 student models use ResNet-50 as the backbone. The left two
 605 images show that 1) the teacher and 2) Zhang et al. [14]’s
 606 model inaccurately predict the truck in the marked cyan oval
 607 boxes. From the zoomed-in view, we can see that both 1) and
 608 2) incorrectly generate two bounding boxes in the truck region
 609 (each with a different category, dark blue: car, light blue: truck).
 610 The reason for the detection issue is that the object is occluded
 611 and the teacher model cannot impart trustworthy information to
 612 the student model in such scenarios. Zhang et al. [14]’s distilled
 613 model blindly trusts the teacher’s prediction and thus makes a
 614 similar mistake. In contrast, our AID-distilled model relies more
 615 on itself when learned to predict for such instances. Thus, only
 616 our model provides the right number of bounding box, of the
 617 right category, and at a precise location (rightmost picture).

618 D. Multi-Teacher Adaptive Distillation (M-AID) Results

619 1) Quantitative Analysis: We employed five teacher detec-
 620 tors of different types to perform M-AID:

- 621 • Generalized Focal Loss (GFL) [53]
- 622 • RetinaNet [17]
- 623 • Adaptive training sample selection (Atss) [69]
- 624 • fully convolutional one-stage (Fcos) [39]
- 625 • GFL [53] with DCONV [70] added

626 Our M-AID experiments were conducted on the KITTI and
 627 COCO-Traffic datasets. We experimented with two GFL student
 628 models: one with a ResNet-50 backbone (named Student-R50)
 629 and the other with a ResNet-18 backbone (named Student-R18).
 630 The quantitative results on the two datasets are shown in
 631 Tables IV and V, respectively. As comparison, single-teacher
 632 student models, i.e., distilled by LD [13] or LD + AID (AID for
 633 short), are also included in the two tables. In Tables IV and V,
 634 the columns denote the teachers, except for the last two columns
 635 where the two students’ mAP performance are shown. The
 636 rows are grouped by the KD method used. Each row represents
 637 a knowledge distillation procedure guided by certain teacher(s).
 638 For reference, we add the teacher models’ mAP performance
 639 under their names. The use of a teacher is marked by a check
 640 under their names. The use of a teacher is marked by a check

641 mark. For example, in our multi-teacher KD case (M-AID),
 642 the two check marks in the bottom row of the two tables
 643 indicate that the two corresponding teachers (GFL and Atss)
 644 jointly guide a student model. It is worth noting that if either
 645 teacher model uses DCONV [70], the student model will also
 646 use it.

647 As shown in Tables IV and V, our instance, scale, and teacher
 648 aware M-AID outperforms the “distillation-free” student-
 649 baseline and the state-of-the-art KD methods (LD [13] and
 650 our AID) in a variety of teacher-student combinations on the
 651 KITTI and COCO-Traffic datasets. For instance, according to
 652 the bottom row of Table IV, we can see that the ResNet-18 based
 653 student model (Student-R18) jointly distilled by the two teachers
 654 (i.e., GFL and Atss) achieves a mAP of 86.8. This mAP score
 655 is higher than separately using either one of the two teachers
 656 (GFL or Atss) to distill the student. According to Table IV, the
 657 same student distilled by the single-teacher AID achieves 83.8
 658 mAP (with Teacher GFL) and 86.1 mAP (with Teacher Atss).
 659 Although the AID results are worse than M-AID’s, they are still
 660 better than Zheng et al.’s LD knowledge distillation results (83.6
 661 mAP using Teacher GFL and 84.5 mAP using Teacher Atss).
 662 On average, there is a 2.93% mAP improvement on KITTI and
 663 2.91% mAP improvement on COCO-Traffic over the student
 664 baseline by using our M-AID. Although, in most cases, M-AID
 665 distilled models can achieve higher performance than those
 666 distilled by AID, exceptions may exist when the performance
 667 gap between the teacher models is large. In such scenarios, we
 668 find that the student can be misled by the worse teacher model.
 669 For example, in Table IV, the student model trained by GFL [53]
 670 and Retina [17] performed no better than the model distilled by
 671 a single GFL teacher using AID.

672 2) Qualitative Analysis: To better understand the distilled
 673 models, we visualize the differences in their focus/attention
 674 using saliency maps. Specifically, we visualize the Eigen Class
 675 Activation Mapping (EigenCAM [71]) of different models’ FPN
 676 neck. The results are shown in Fig. 5.

677 According to Fig. 5, in image A, the “distillation-free” model
 678 focuses on the object’s surroundings, but has a low attention
 679 overlap with the object. It incorrectly detects the fence as a car.

TABLE IV
RESULTS OF MULTI-TEACHER EXPERIMENTS ON THE KITTI DATASET

KD methods \ Teacher Models (w ResNet-101)	GFL [53]	GFL-dconv [70]	Retina [17]	Fcos [39]	Atss [69]	Student-R50	Student-R18
	89.4	88.8	84.8	88.3	88.7	85.1	81.9
Student-baseline		✓				87.1	83.0
			✓		✓	82.9	79.4
				✓		75.4	79.2
					✓	85.4	82.6
LD [13]	✓	✓				85.5	83.6
			✓		✓	85.5	84.6
				✓		83.7	82.2
					✓	76.9	81.1
						86.1	84.5
AID	✓	✓				87.2	83.8
			✓		✓	87.1	85.1
				✓		85.4	84.4
					✓	81.2	82.0
						87.3	86.1
M-AID	✓	✓				88.0	85.8
	✓				✓	86.1	85.6
	✓					86.6	84.8
	✓					87.7	86.8

Note: each row represents a knowledge distillation procedure guided by certain teacher(s). The use of a teacher is marked by a check mark. For our multi-teacher approach (M-AID), the two check marks in a row indicate that the two corresponding teachers jointly guide a student model. We have tested on two student models. Student-R50 stands for a student model with a ResNet-50 backbone. Student-R18 is similarly defined. Their mAP performance are appended to the table as the last two columns. For reference, we add the teacher models' mAP performance under their names. AID and M-AID are applied on top of LD. GFL-dconv stands for a GFL model with the deformable convolutional networks [70] trick added. The student-baseline is the certain detector without applying any distillation method.

TABLE V
RESULTS OF MULTI-TEACHER EXPERIMENTS ON THE COCO-TRAFFIC DATASET

KD methods \ Teacher Models (w ResNet-101)	GFL [53]	GFL-dconv [70]	Retina [17]	Fcos [39]	Atss [69]	Student-R50	Student-R18
	71.8	73.8	68.9	72.7	72.7	67.7	61.9
Student-baseline		✓				72.0	63.5
			✓		✓	66.7	59.7
						59.8	59.8
					✓	67.4	62.2
LD [13]	✓	✓				67.8	62.7
			✓		✓	72.5	64.3
				✓		67.8	61.3
					✓	67.3	61.9
						68.7	63.9
AID	✓	✓				68.4	64.4
			✓		✓	72.3	65.7
				✓		68.6	62.8
					✓	67.8	63.6
						69.8	64.2
M-AID	✓	✓				72.8	65.9
	✓				✓	69.5	63.8
	✓					69.7	64.9
	✓					70.0	65.1

Note: each row represents a knowledge distillation procedure guided by certain teacher(s). The use of a teacher is marked by a check mark. For our multi-teacher approach (M-AID), the two check marks in a row indicate that the two corresponding teachers jointly guide a student model. We have tested on two student models. Student-R50 stands for a student model with a ResNet-50 backbone. Student-R18 is similarly defined. Their mAP performance are appended to the table as the last two columns. For reference, we add the teacher models' mAP performance under their names. AID and M-AID are applied on top of LD. GFL-dconv stands for a GFL model with the deformable convolutional networks [70] trick added. The student-baseline is the certain detector without applying any distillation method.

We can see that LD [13] does improve the model's attention, but still produces false detection on the fence. Our AID and M-AID both succeed in avoiding the detection mistake. However, only our M-AID distillation model pays attention to the full body of the car on the bottom left of the image, and the M-AID model achieves the highest mAP.

Similarly, from Fig. 5's image B, we can see that AID improves the model's ability to detect occluded objects. Our M-AID further optimizes the attention of the model and its ability to detect small and overlapping objects. For example, in image B, the AID and M-AID models successfully detect the partially occluded car behind the one closest to the camera. The

red attention area of M-AID covers more pixels of the partially occluded car. Moreover, the M-AID model is the only one that succeeds to detect each of the three overlapping cars at the far end of image B.

E. Computational Complexity

In addition to mAP performance, we also compared different architectures' efficiency in terms of FLOPs⁴ and

⁴In the DL literature, there are two FLOP versions: 1) multiply-and-add (e.g., [13]), and 2) multiply/add (e.g., [72]). We follow the former convention.

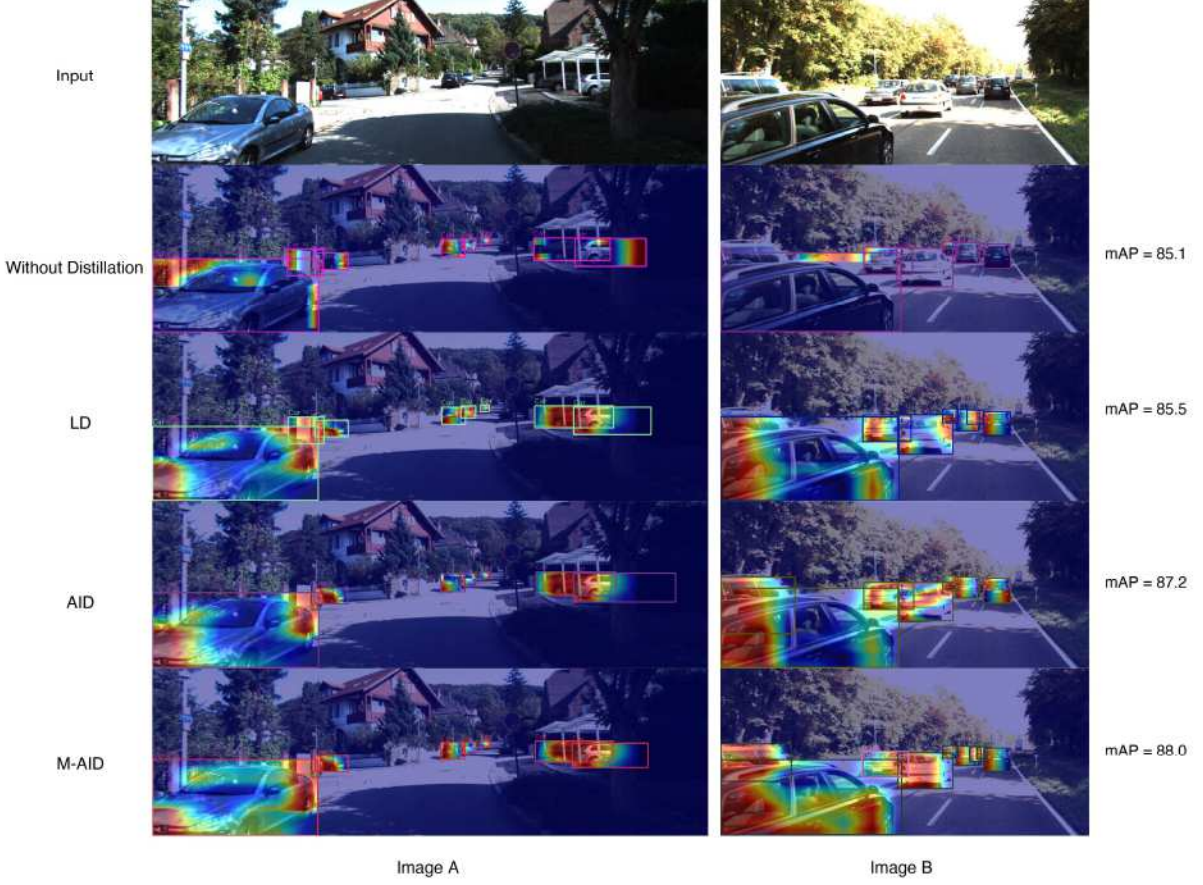


Fig. 5. Attention maps of student models distilled by the state-of-the-art LD, our AID and M-AID methods. We show the CAM saliency of the different student models' FPN neck with ResNet-50 as backbone. Different colors indicate different attention levels, with the red color representing the highest attention and the blue color representing the lowest. The dark red regions contribute most to model decision. Best viewed in color and zoomed in.

TABLE VI
MODEL COMPLEXITY (WITH 224×224 INPUT RESOLUTION)

Model	Backbones	Parames(M)	GFLOPs
GFL [53]	ResNet-101	51.03	13.79
	ResNet-50	32.04	10.05
	ResNet-18	19.09	7.61
ATSS [69]	ResNet-101	51.03	13.78
	ResNet-50	32.04	10.05
	ResNet-18	19.09	7.62
FCOS [39]	ResNet-101	55.06	13.61
	ResNet-50	36.12	9.88
	ResNet-18	19.67	7.63
Retina [17]	ResNet-101	55.35	14.04
	ResNet-50	36.15	10.09
	ResNet-18	19.66	7.60
GFL-Dconv [70]	ResNet-101	52.32	10.57
	ResNet-50	32.62	8.67
	ResNet-18	19.38	6.98
Faster R-CNN [33]	ResNet-101	60.13	27.09
	ResNet-50	41.13	23.36
	ResNet-18	28.13	20.77
PAA [26]	ResNet-101	50.89	13.63
	MobileNetV2	10.28	5.95

parameters. The results are shown in Table VI. According to the table, our distilled models with the smaller backbones (ResNet-50, ResNet-18, or MobileNetV2) are more efficient than the corresponding teacher baselines with larger ResNet-101 backbones. In addition to the previously mentioned promising

mAPs, our ResNet-18/50 distillation model enjoys an average of 61.68%/35.46% reduction in the number of parameters and an average of 39.31%/22.69% savings in FLOPs. The MobileNetV2 can achieve 79.80% reduction of parameters and 56.35% saving in FLOPs.

V. CONCLUSION

In this paper, we have proposed adaptive instance distillation (AID) and multi-teacher adaptive instance distillation (M-AID) methods to derive more compact and better-performing visual detectors for self-driving vehicles. The AID method redirects more student attention to instances that the teacher model performs well on. Our M-AID empowers the student model to learn more from more knowledgeable teachers w.r.t an instance and a scale. For the first time, we guide the student detector to actively search for valuable knowledge across different instances, teachers, and scales during distillation. In our experiments, we have compared our methods with a wide array of state-of-the-art knowledge distillation baselines (e.g., [11], [12], [13], [14], [15], [16], [21], [25]) and have tested our strategies using both single-stage and double-stage detectors. Experimental results on the KITTI, COCO-Traffic, and SODA10 M datasets demonstrate our AID and M-AID methods' efficacy. On average, 2.28% and 2.98% mAP increases can be achieved by AID for the

single-stage detectors and two-stage detectors, respectively. Furthermore, our M-AID method leads to an average of 2.92% mAP improvement.

ACKNOWLEDGMENT

This work would not have been possible without the computing resources provided by the Ohio Supercomputer Center.

REFERENCES

- [1] C. Chen, A. Seff, A. Kornhauser, and J. Xiao, "DeepDriving: Learning affordance for direct perception in autonomous driving," in *Proc. IEEE Int. Conf. Comput. Vis.*, 2015, pp. 2722–2730.
- [2] M. Bojarski et al., "End to end learning for self-driving cars," 2016, *arXiv:1604.07316*.
- [3] Z. Chen and X. Huang, "End-to-end learning for lane keeping of self-driving cars," in *Proc. IEEE Intell. Veh. Symp.*, 2017, pp. 1856–1860.
- [4] H. Xu, Y. Gao, F. Yu, and T. Darrell, "End-to-end learning of driving models from large-scale video datasets," in *Proc. IEEE Conf. Comput. Vis. Pattern Recognit.*, 2017, pp. 3530–3538.
- [5] Z. Rozsa and T. Sziranyi, "Object detection from a few LIDAR scanning planes," *IEEE Trans. Intell. Veh.*, vol. 4, no. 4, pp. 548–560, Dec. 2019.
- [6] J. E. Hoffmann, H. G. Tosso, M. M. D. Santos, J. F. Justo, A. W. Malik, and A. U. Rahman, "Real-time adaptive object detection and tracking for autonomous vehicles," *IEEE Trans. Intell. Veh.*, vol. 6, no. 3, pp. 450–459, Sep. 2021.
- [7] M. Schutera, M. Hussein, J. Abhau, R. Mikut, and M. Reischl, "Night-to-day: Online image-to-image translation for object detection within autonomous driving by night," *IEEE Trans. Intell. Veh.*, vol. 6, no. 3, pp. 480–489, Sep. 2021.
- [8] J. I. Choi and Q. Tian, "Adversarial attack and defense of YOLO detectors in autonomous driving scenarios," in *Proc. IEEE Intell. Veh. Symp.*, 2022, pp. 1011–1017.
- [9] G. Hinton, O. Vinyals, and J. Dean, "Distilling the knowledge in a neural network," 2015, *arXiv:1503.02531*.
- [10] A. Krizhevsky and G. Hinton, "Learning multiple layers of features from tiny images," Master's thesis, Dept. Comput. Sci., Univ. Toronto, 2009.
- [11] T. Wang, L. Yuan, X. Zhang, and J. Feng, "Distilling object detectors with fine-grained feature imitation," in *Proc. IEEE/CVF Conf. Comput. Vis. Pattern Recognit.*, 2019, pp. 4928–4937.
- [12] J. Guo et al., "Distilling object detectors via decoupled features," in *Proc. IEEE/CVF Conf. Comput. Vis. Pattern Recognit.*, 2021, pp. 2154–2164.
- [13] Z. Zheng et al., "Localization distillation for dense object detection," in *Proc. IEEE/CVF Conf. Comput. Vis. Pattern Recognit.*, 2022, pp. 9397–9406.
- [14] L. Zhang and K. Ma, "Improve object detection with feature-based knowledge distillation: Towards accurate and efficient detectors," in *Proc. Int. Conf. Learn. Representations*, 2021. [Online]. Available: <https://openreview.net/forum?id=uKhGRvM8QNH>
- [15] Z. Yang et al., "Focal and global knowledge distillation for detectors," in *Proc. IEEE/CVF Conf. Comput. Vis. Pattern Recognit.*, 2022, pp. 4633–4642.
- [16] X. Dai et al., "General instance distillation for object detection," in *Proc. IEEE/CVF Conf. Comput. Vis. Pattern Recognit.*, 2021, pp. 7838–7847.
- [17] T.-Y. Lin, P. Goyal, R. Girshick, K. He, and P. Dollár, "Focal loss for dense object detection," in *Proc. IEEE Int. Conf. Comput. Vis.*, 2017, pp. 2999–3007.
- [18] B. Li, Y. Liu, and X. Wang, "Gradient harmonized single-stage detector," in *Proc. AAAI Conf. Artif. Intell.*, 2019, pp. 8577–8584.
- [19] Y. Cao, K. Chen, C. C. Loy, and D. Lin, "Prime sample attention in object detection," in *Proc. IEEE/CVF Conf. Comput. Vis. Pattern Recognit.*, 2020, pp. 11580–11588.
- [20] W. Liu et al., "SSD: Single shot multibox detector," in *Proc. Eur. Conf. Comput. Vis.*, 2016, pp. 21–37.
- [21] Y. Zhang et al., "Prime-aware adaptive distillation," in *Proc. Eur. Conf. Comput. Vis.*, 2020, pp. 658–674.
- [22] S. You, C. Xu, C. Xu, and D. Tao, "Learning from multiple teacher networks," in *Proc. 23rd ACM SIGKDD Int. Conf. Knowl. Discov. Data Mining*, 2017, pp. 1285–1294.
- [23] Y. Liu, W. Zhang, and J. Wang, "Adaptive multi-teacher multi-level knowledge distillation," *Neurocomputing*, vol. 415, pp. 106–113, 2020.
- [24] Q. Lan and Q. Tian, "Adaptive instance distillation for object detection in autonomous driving," in *Proc. Int. Conf. Pattern Recognit.*, 2022.
- [25] C. H. Nguyen, T. C. Nguyen, T. N. Tang, and N. L. Phan, "Improving object detection by label assignment distillation," in *Proc. IEEE/CVF Winter Conf. Appl. Comput. Vis.*, 2022, pp. 1322–1331.
- [26] K. Kim and H. S. Lee, "Probabilistic anchor assignment with IoU prediction for object detection," in *Proc. Eur. Conf. Comput. Vis.*, 2020, pp. 355–371.
- [27] M. Sandler, A. Howard, M. Zhu, A. Zhmoginov, and L.-C. Chen, "MobileNetV2: Inverted residuals and linear bottlenecks," in *Proc. IEEE Conf. Comput. Vis. Pattern Recognit.*, 2018, pp. 4510–4520.
- [28] J. Han et al., "SODA10M: A large-scale 2D self/semi-supervised object detection dataset for autonomous driving," 2021, *arXiv:2106.11118*.
- [29] Transitioning to tesla vision. Accessed: Aug. 19, 2022. [Online]. Available: <https://www.tesla.com/support/transitioning-tesla-vision>
- [30] Tesla commits to pure vision approach, removes radar from model S and model X. Accessed: Feb. 25, 2022. [Online]. Available: <https://www.teslarati.com/tesla-commits-pure-vision-approach-model-s-model-x-no-radar/>
- [31] R. Vaillant, C. Monrocq, and Y. L. Cun, "An original approach for the localization of objects in images," in *Proc. 3rd Int. Conf. Artif. Neural Netw.*, 1993, pp. 26–30.
- [32] P. Viola and M. Jones, "Rapid object detection using a boosted cascade of simple features," in *Proc. IEEE Comput. Soc. Conf. Comput. Vis. Pattern Recognit.*, 2001, pp. I–I.
- [33] S. Ren, K. He, R. Girshick, and J. Sun, "Faster R-CNN: Towards real-time object detection with region proposal networks," in *Proc. Int. Conf. Neural Inf. Process. Syst.*, 2015, pp. 91–99.
- [34] Z. Cai and N. Vasconcelos, "Cascade R-CNN: Delving into high quality object detection," in *Proc. IEEE Conf. Comput. Vis. Pattern Recognit.*, 2018, pp. 6154–6162.
- [35] K. He, G. Gkioxari, P. Dollár, and R. Girshick, "Mask R-CNN," in *Proc. IEEE Int. Conf. Comput. Vis.*, 2017, pp. 2980–2988.
- [36] J. Redmon and A. Farhadi, "YOLO9000: Better, faster, stronger," in *Proc. IEEE Conf. Comput. Vis. Pattern Recognit.*, 2017, pp. 6517–6525.
- [37] J. Redmon and A. Farhadi, "YOLOv3: An incremental improvement," 2018, *arXiv:1804.02767*.
- [38] Z. Ge, S. Liu, F. Wang, Z. Li, and J. Sun, "YOLOX: Exceeding YOLO series in 2021," 2021, *arXiv:2107.08430*.
- [39] Z. Tian, C. Shen, H. Chen, and T. He, "FCOS: Fully convolutional one-stage object detection," in *Proc. IEEE/CVF Int. Conf. Comput. Vis.*, 2019, pp. 9626–9635.
- [40] Z. Yang, S. Liu, H. Hu, L. Wang, and S. Lin, "RepPoints: Point set representation for object detection," in *Proc. Int. Conf. Comput. Vis.*, 2019, pp. 9656–9665. [Online]. Available: <https://www.microsoft.com/en-us/research/publication/reppoints-point-set-representation-for-object-detection/>
- [41] K. Duan, S. Bai, L. Xie, H. Qi, Q. Huang, and Q. Tian, "CenterNet: Keypoint triplets for object detection," in *Proc. IEEE/CVF Int. Conf. Comput. Vis.*, 2019, pp. 6568–6577.
- [42] T.-Y. Lin, P. Dollár, R. Girshick, K. He, B. Hariharan, and S. Belongie, "Feature pyramid networks for object detection," in *Proc. IEEE Conf. Comput. Vis. Pattern Recognit.*, 2017, pp. 936–944.
- [43] S. Qiao, L.-C. Chen, and A. Yuille, "DetectoRS: Detecting objects with recursive feature pyramid and switchable atrous convolution," in *Proc. IEEE/CVF Conf. Comput. Vis. Pattern Recognit.*, 2021, pp. 10208–10219.
- [44] A. Romero et al., "FitNets: Hints for thin deep nets," in *Proc. Int. Conf. Learn. Representations*, 2015.
- [45] Z. Huang and N. Wang, "Like what you like: Knowledge distill via neuron selectivity transfer," 2017, *arXiv:1707.01219*.
- [46] S. Ahn, S. X. Hu, A. Damianou, N. D. Lawrence, and Z. Dai, "Variational information distillation for knowledge transfer," in *Proc. IEEE/CVF Conf. Comput. Vis. Pattern Recognit.*, 2019, pp. 9155–9163.
- [47] B. Heo, M. Lee, S. Yun, and J. Y. Choi, "Knowledge transfer via distillation of activation boundaries formed by hidden neurons," in *Proc. AAAI Conf. Artif. Intell.*, 2019, pp. 3779–3787.
- [48] J. Yim, D. Joo, J. Bae, and J. Kim, "A gift from knowledge distillation: Fast optimization, network minimization and transfer learning," in *Proc. IEEE Conf. Comput. Vis. Pattern Recognit.*, 2017, pp. 7130–7138.

794
795
796
797
798
799
800
801
802
803
804
805
806
807
808
809
810
811
812
813
814
815
816
817
818
819
820
821
822
823
824
825
826
827
828
829
830
831
832
833
834
835
836
837
838
839
840
841
842
843
844
845
846
847
848
849
850
851
852
853
854
855
856
857
858
859
860
861
862
863
864
865
866

867 [49] Y. Liu et al., "Knowledge distillation via instance relationship graph,"
868 in *Proc. IEEE/CVF Conf. Comput. Vis. Pattern Recognit.*, 2019,
869 pp. 7089–7097.

870 [50] W. Park, D. Kim, Y. Lu, and M. Cho, "Relational knowledge distilla-
871 tion," in *Proc. IEEE/CVF Conf. Comput. Vis. Pattern Recognit.*, 2019,
872 pp. 3962–3971.

873 [51] G. Chen, W. Choi, X. Yu, T. Han, and M. Chandraker, "Learning efficient
874 object detection models with knowledge distillation," in *Proc. Int. Conf.
875 Neural Inf. Process. Syst.*, 2017, pp. 742–751.

876 [52] M. Hao, Y. Liu, X. Zhang, and J. Sun, "LabelEnc: A new intermediate
877 supervision method for object detection," in *Proc. Eur. Conf. Comput.
878 Vis.*, 2020, pp. 529–545.

879 [53] X. Li et al., "Generalized focal loss: Learning qualified and distributed
880 bounding boxes for dense object detection," in *Proc. Int. Conf. Neural Inf.
881 Process. Syst.*, 2020, pp. 21002–21012.

882 [54] J. Deng, Y. Pan, T. Yao, W. Zhou, H. Li, and T. Mei, "Relation distilla-
883 tion networks for video object detection," in *Proc. IEEE/CVF Int. Conf.
884 Comput. Vis.*, 2019, pp. 7022–7031.

885 [55] L. F. Zeni and C. R. Jung, "Distilling knowledge from refinement in
886 multiple instance detection networks," in *Proc. IEEE/CVF Conf. Comput.
887 Vis. Pattern Recognit. Workshops*, 2020, pp. 3324–3333.

888 [56] H. Zhang, D. Chen, and C. Wang, "Confidence-aware multi-teacher knowl-
889 edge distillation," in *Proc. IEEE Int. Conf. Acoust. Speech Signal Process.*,
890 2022, pp. 4498–4502.

891 [57] T. Fukuda, M. Suzuki, G. Kurata, S. Thomas, J. Cui, and B. Ramabhadran,
892 "Efficient knowledge distillation from an ensemble of teachers," in *Proc.
893 18th Annu. Conf. Int. Speech Commun. Assoc.*, 2017, pp. 3697–3701.

894 [58] S. Du et al., "Agree to disagree: Adaptive ensemble knowledge distil-
895 lation in gradient space," in *Proc. Int. Conf. Neural Inf. Process. Syst.*,
896 2020, pp. 12345–12355. [Online]. Available: <https://proceedings.neurips.cc/paper/2020/file/91c77393975889bd08f301c9e13a44b7-Paper.pdf>

897 [59] S. You, C. Xu, C. Xu, and D. Tao, "Learning with single-teacher multi-
898 student," in *Proc. AAAI Conf. Artif. Intell.*, 2018, pp. 4390–4397.

899 [60] X. Zhu et al., "Knowledge distillation by on-the-fly native ensemble," in
900 *Proc. Int. Conf. Neural Inf. Process. Syst.*, 2018, pp. 7528–7538.

901 [61] D. Chen, J.-P. Mei, C. Wang, Y. Feng, and C. Chen, "Online knowledge
902 distillation with diverse peers," in *Proc. AAAI Conf. Artif. Intell.*, 2020,
903 pp. 3430–3437.

904 [62] L. Tran et al., "Hydra: Preserving ensemble diversity for model distilla-
905 tion," 2020, *arXiv:2001.04694*.

906 [63] A. Geiger, P. Lenz, and R. Urtasun, "Are we ready for autonomous driving?
907 The KITTI vision benchmark suite," in *Proc. IEEE Conf. Comput. Vis.
908 Pattern Recognit.*, 2012, pp. 3354–3361.

909 [64] SSD: Single shot MultiBox detector—train the KITTI dataset,
910 Mar. 2017. [Online]. Available: [https://blog.csdn.net/jesse_mx/article/
912 details/65634482](https://blog.csdn.net/jesse_mx/article/
911 details/65634482)

913 [65] T.-Y. Lin et al., "Microsoft COCO: Common objects in context," in *Proc.
914 Eur. Conf. Comput. Vis.*, 2014, pp. 740–755.

915 [66] K. He, X. Zhang, S. Ren, and J. Sun, "Deep residual learning for image
916 recognition," in *Proc. IEEE Conf. Comput. Vis. Pattern Recognit.*, 2016,
917 pp. 770–778.

[67] K. Chen et al., "MMDetection: Open MMLab detection toolbox and
918 benchmark," 2019, *arXiv:1906.07155*.

[68] A. Paszke et al., "PyTorch: An imperative style, high-performance deep
919 learning library," in *Proc. 33rd Int. Conf. Neural Inf. Process. Syst.*, 2019,
920 Art. no. 721.

[69] S. Zhang, C. Chi, Y. Yao, Z. Lei, and S. Z. Li, "Bridging the gap between
921 anchor-based and anchor-free detection via adaptive training sample se-
922 lection," in *Proc. IEEE/CVF Conf. Comput. Vis. Pattern Recognit.*, 2020,
923 pp. 9756–9765.

[70] J. Dai et al., "Deformable convolutional networks," in *Proc. IEEE Int.
924 Conf. Comput. Vis.*, 2017, pp. 764–773.

[71] M. B. Muhammad and M. Yesin, "Eigen-CAM: Class activation map
925 using principal components," in *Proc. Int. Joint Conf. Neural Netw.*, 2020,
926 pp. 1–7.

[72] Q. Tian, T. Arbel, and J. J. Clark, "Task dependent deep LDA pruning
927 of neural networks," *Comput. Vis. Image Understanding*, vol. 203, 2021,
928 Art. no. 103154.



Qizhen Lan received the bachelor's degree in information management and information systems from Tiangong University, Tianjin, China, in 2018, the bachelor's degree in business analytics in 2018, the master's degree in intelligence and analytics in 2019 both from the Bowling Green State University, Bowling Green, OH, USA, where he is currently working toward the Ph.D. degree in data science. His research interests include knowledge distillation, deep network pruning, and visual detection of autonomous vehicles.



Qing Tian received the B.Eng. degree in computer science and engineering from Yanshan University, Qinhuangdao, Hebei, China, in 2011, the M.Eng. and Ph.D. degrees in electrical engineering from McGill University, Montreal, QC, Canada in 2013 and 2021, respectively. He is currently an Assistant Professor with Bowling Green State University, Bowling Green, OH, USA. From 2019 to 2020, he was an Applied Scientist Intern with Amazon.com Inc. (Visual Search & AR), Palo Alto, CA, USA. From 2013 to 2014, he was a Software Developer with Nakisa Inc., Montreal, QC, Canada. His research interests include deep neural network compression, efficient neural architecture search, and adversarial AI. His current project in efficient and trustworthy self-driving visual perception is supported by the National Science Foundation.